SKBF KBS TECHNICAL REPORT 83-27

Radiation effects on the chemical environment in a radioactive waste repository

Tryggve E Eriksen

Royal Institute of Technology, Stockholm

Arvid Jacobsson

University of Luleå, Luleå
Sweden 1983-07-01

SVENSK KÄRNBRÄNSLEFÖRSÖRJNING AB / AVDELNING KBS
Swedish Nuclear Fuel Supply Co/Division KBS
MAILING ADDRESS: SKBF/KBS, Box 5864, S-102 48 Stockholm, Sweden
Telephone 08-67 95 40

RADIATION EFFECTS ON THE CHEMICAL ENVIRONMENT IN A RADIOACTIVE WASTE REPOSITORY

Trygve Eriksen
Royal Institute of Technology, Stockholm

Arvid Jacobsson
University of Luleå, Luleå

Sweden 1983-07-01

A list of other reports published in this series during 1983 is attached at the end of this report. Information on KBS technical reports from 1977-1978 (TR 121), 1979 (TR 79-28), 1980 (TR 80-26), 1981 (TR 81-17) and 1982 (TR 82-28) is available through SKBF/KBS.

Radiation effects on the chemical environment in a radioactive waste repository.

Trygve E Eriksen [1] and Arvid Jacobsson [2]

[1] Department of Nuclear Chemistry, the Royal Institute of Technology, 100 44 Stockholm, Sweden.

[2] Division Soil Mechanics, University of Luleå, 951 87 Luleå, Sweden.

CONTENTS

SUMMARY

The radiolytic hydrogen production in compacted bentonite have been measured at two dose rates 6.1 and 0.014 rad·sec^{-1}. The hydrogen production depends on the Fe^{2+} and HCO_3^- concentration in the pore water and on the dose rate. The hydrogen production at 6.1 rad·sec^{-1} is in agreement with the hydrogen production calculated assuming homogeneous kinetics and Fe^{2+} and HCO_3^- concentrations of $2.2 \cdot 10^{-7}$ and $6.5 \cdot 10^{-5}$ mol·dm^{-3} respectively. The amount of divalent iron in the bentonite clay accessible for scavenging of oxidative radicals was found by Mössbauer spectroscopy to be at least 0.4%.

1 INTRODUCTION

Although the direct effect of β^- and γ radiations on the backfill material (bentonite) in a repository for nuclear waste is expected to be small (1), radiolysis of the pore water may greatly change the redox properties of the immediate environment of the waste canisters. The primary oxidizing and reducing species formed upon radiolysis of water will react with solute species and the redox-potential is therefore strongly dependent on the pore water composition.

Using a homogeneous reaction model H Christensen (2) have carried out computer calculations of the radiolysis and obtained steady state concentrations of hydrogen peroxide (H_2O_2) and hydrogen (H_2) (2,3). The calculated steady state concentrations were found to be in good agreement with experimental data obtained by Eriksen and Lind (4).

Due to its low reactivity H_2 may diffuse away and thereby create a migrating redox front as proposed by Neretnieks (5). A number of computer calculations taking into account the diffusion of H_2 have been carried out by Christensen and Bjergbakke (6). An important solute in ground water is the Fe^{2+} ion as this is a good scavenger of oxidizing radicals. The product Fe^{3+} has much lower solubility at the environmental pH and precipitates.The Fe^{2+} concentration in the water is thus as demonstrated by the computer calculations,of great importance for the H_2 production. Also, as the formation of a moving redox front is caused by the oxidative depletion of divalent iron in the bentonite backfill and the surrounding rock knowledge of the total accessible Fe(II) content is important.

The present report deals with the diffusion of H_2 away from a well defined β^- irradiated volume of compacted watersaturated bentonite. The experimental results are compared with the H_2 production calculated by the kinetic model used by Christensen and Bjerkbakke. Due to the importance of the total accessible Fe(II) content as a sink for oxidizing radicals in the bentonite, this report also deals with leaching of Fe^{2+} and Mössbauer analysis of iron in the bentonite.

2 EXPERIMENTAL.

2.1 RADIOLYSIS.

The bentonite used in the present study was the American Colloid Co type MX-80 granulated Na bentonite. The irradiations were carried out in swelling pressure oedometers build at the University of Luleå (figures 1,2).

In the experiments discussed in this report compacted clay was equilibrated with a synthetic ground water solution. In a previous experiment the desired amount of water as finely ground ice prepared from deoxygenated distilled water was mixed thoroughly with bentonite at low temperature (4). The radiations used in the high dose experiments were low energy β^- (Pm-147) (E_{max} = 225 keV) and γ (Co-60) respectively. Two oedometers with different irradiation geometries were used. The bentonite was compacted under nitrogen (N_2) atmosphere to desired density and thereafter contacted with N_2 purged water for 2-3 weeks.

2.1.1 Beta source experiments

After water saturation, the oedometer according to figure 1 was opened and a 200 mCi extended area Pm-147 source mounted as shown the figure thereby obtaining a well defined irradiation volume and diffusion distance. The oedometer was therafter connected to a gaschromotograph and the H_2 diffusing through the 14 mm thick bentonite cylinder measured at differing times after the onset of irradiation.

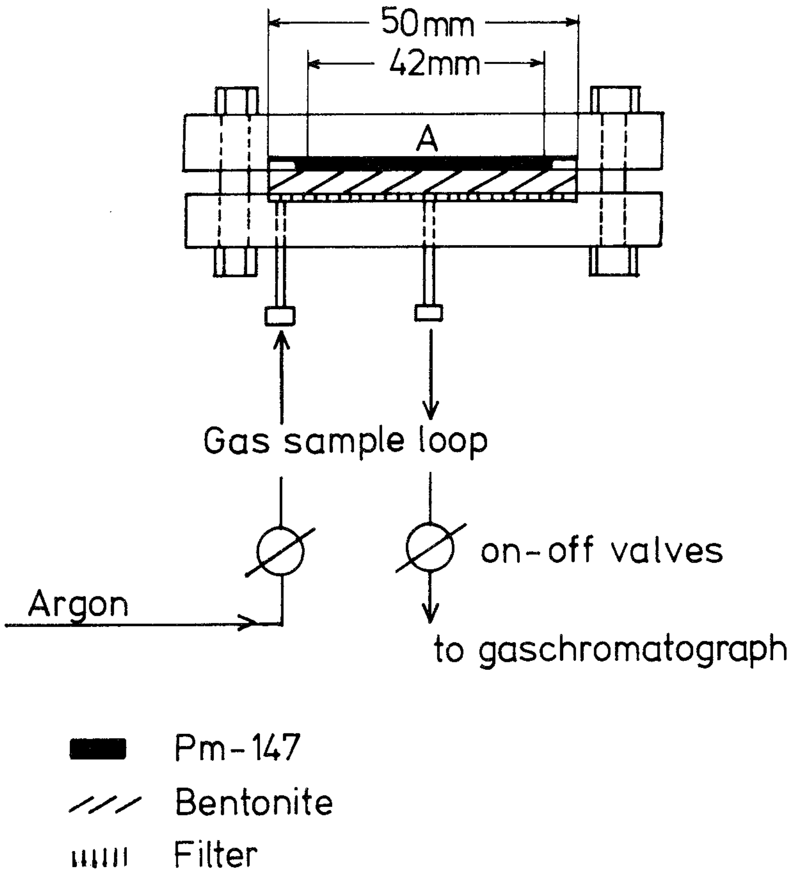

Fig. 1
Schematic drawing of Pm-147 irradiation cell.

The decay characteristics of the β^- emitting Pm-147 are $t_{1/2}$ = 2.5 y and E_{max} = 225 keV. The calculated relative β^- fluxes versus distance from the Pm-147 foil in water and compacted bentonite (ρ = 2.1 kg·dm^{-3}) are plotted in figure 2.

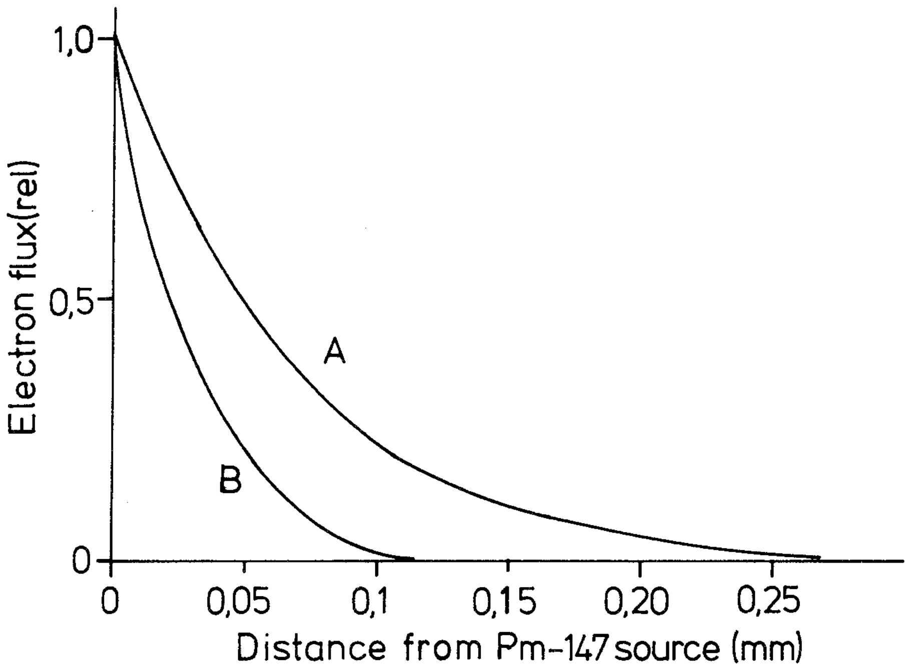

Fig. 2
Relative β^- flux as function of distance from Pm-147 source.
A-water; B-Bentonite
$p = 2.1\ g\cdot cm^{-3}$

As seen in water all the β^- energy is deposited within a distance of 0.25 mm from the radiation source, i.e. in a volume of 0.35 cm^3. The dose was determined by immersing the Pm-147 source in aqueous solution of MeOH (0.5 $mol\cdot dm^{-3}$, pH 5).

The reaction taking place are:

$$e^-_{aq} + H^+ \longrightarrow H\cdot$$

$$OH + CH_3OH \longrightarrow H_2O + \cdot CH_2OH$$

$$H + CH_3OH \longrightarrow H_2 + \cdot CH_2OH$$

$$2\cdot CH_2OH \longrightarrow (CH_2OH)_2$$

and the G-value for H_2 production

$$G(H_2) = G_{H_2} + G_{e^-_{aq}} + G_{H\cdot} = 3.65 \text{ molecules/100 eV absorbed energy}$$

The H_2 production was found to be $0.28\cdot10^{-7}$ mol·h^{-1} and the average dose rate within the irradiated volume thus 6.11 rad·sec^{-1}.

2.1.2 Gamma source experiment

A cylindrical 100 mCi Cs-137 γ-source was inserted into the oedometer as shown in figure 3 and the H_2-concentration at radiolytic equilibrium measured gaschromotographically.

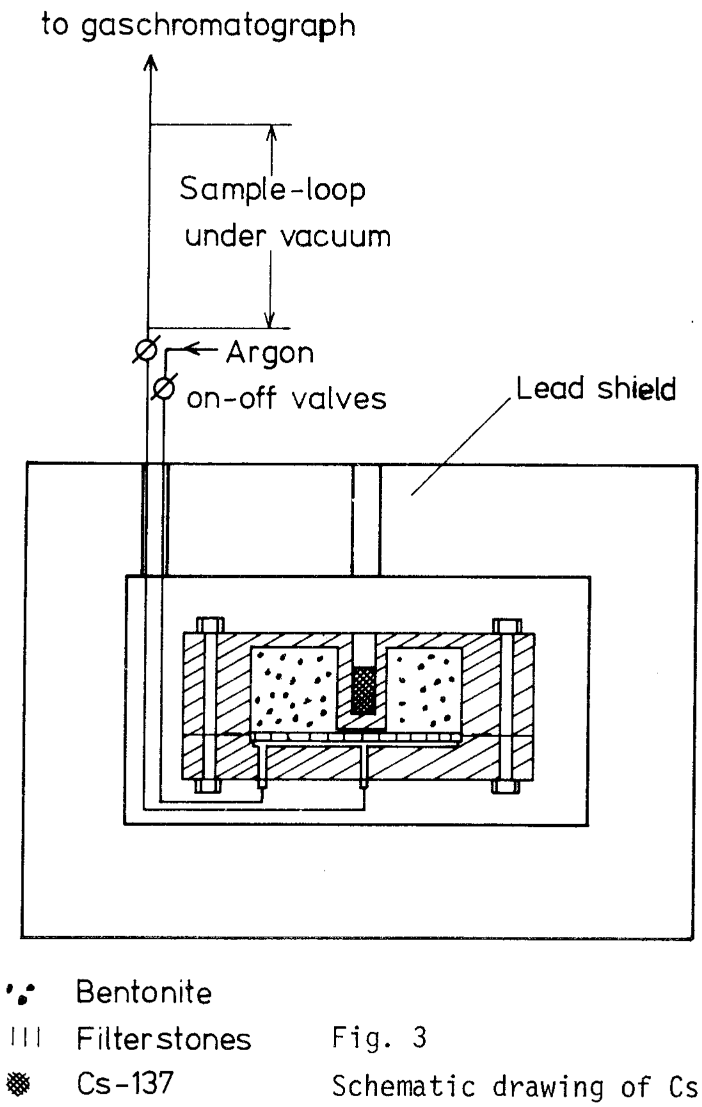

Fig. 3
Schematic drawing of Cs-137 irradiation cell.

The dose rate of the Cs-137-source was measured using the Fricke dosimeter. Assuming $G(Fe^{3+})$ and $\varepsilon(Fe^{3+})$ to be 15.6 and 2197 M^{-1} cm^{-1} (7) respectively the average dose rate was found to be $1.42 \cdot 10^{-2}$ $rad \cdot sec^{-1}$.

2.2 ANALYSIS OF AVAILABLE IRON (II) IN BENTONITE

2.2.1 Leaching experiments

Slightly acid pH ~ 6.5 (HCl) aqueous bentonite suspensions with varyir clay/water ratio were shaken for 30 min. The solid was thereafter separated from the aqueous phase by centrifugation at 2000 rpm and the Fe^{2+} concentration in the water phase determined with o-phenanthroline by the colorometric procedure described in references (8,9) below.

Corresponding experiments were also carried out with clay suspensions 0.5 N $CaCl_2$ (pH ~ 6.5) solutions.

2.2.2 Mössbauer spectroscopy

A constant acceleration Mössbauer spectrometer with horizontal transmission geometry was used. Spectra were recorded at ambient temperature and calibrated by use of an iron foil. Spectra were fitted by a least square method assuming Lorentzian lineshape.

MX-80 bentonite samples were analyzed after the following treatment; as received, addition of 20% (by weight) H_2O, air dried after addition of 20% H_2O; dried at 60^oC for 6h after addition of 20% H_2O, dried for two weeks at room temperature after addition of 20% H_2O, contacted with synthetic ground water for one year in a swelling pressure oedometer.

3 RESULTS AND DISCUSSIONS

3.1 BETA SOURCE

The rate of hydrogen diffusion out of the oedometer containing the Pm-147 foil as a function of irradiation time is shown in figure 4.

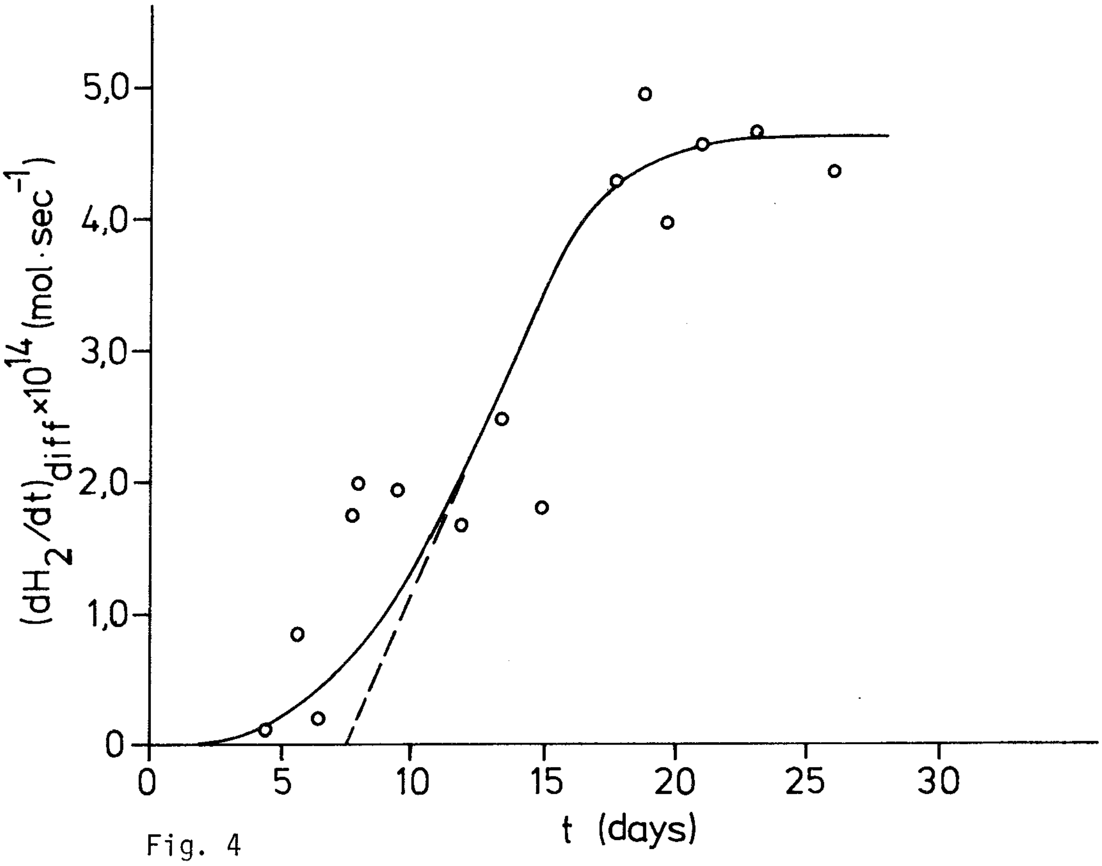

Fig. 4
Hydrogen diffusion out of oedometer containing 200 mCi Pm-147 as function of time after onset of diffusion.
Dose rate ~ 6 rad·sec^{-1}

As shown in figure 2 the β^- energy is deposited within 0.12 mm distance from the Pm-147 source. The concentration profiles of H_2 in the bentonite at three irradiation times calculated from the expression C/C_0 = erfc $(X/2\sqrt{\bar{D}t})$ with $\bar{D} = 4.1 \cdot 10^{-7} cm^2 \cdot sec$, assuming instantaneous radiolysis equilibrium, are plotted in figure 5 (for details on diffusion parameters, see appendix 1).

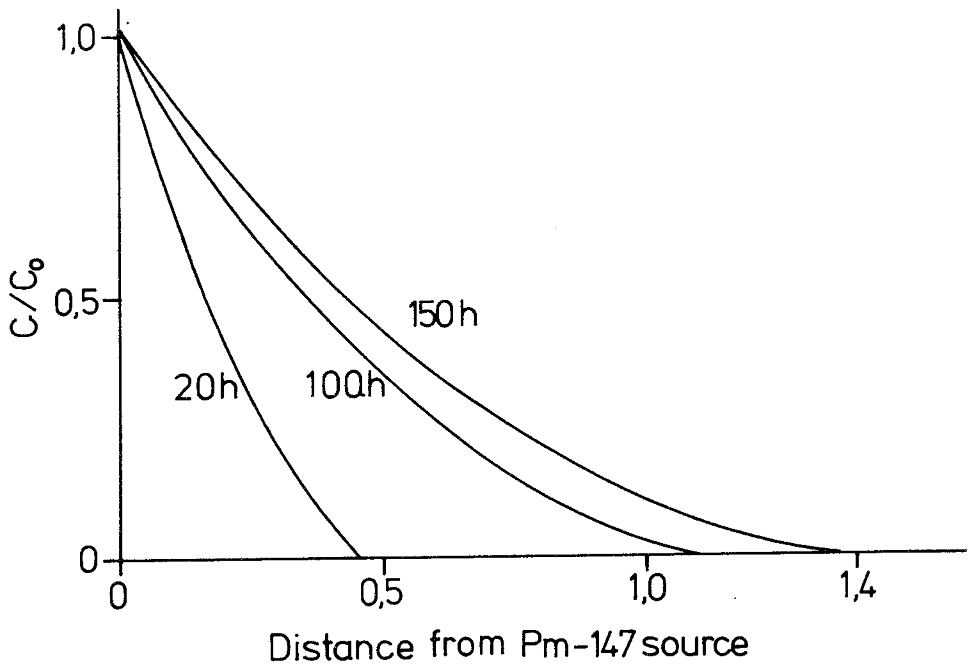

Fig. 5
Expected concentration profile of H_2 at various times after onset of irradiation calculated using the eqn $C/C_0 = \text{erfc}(x/2\sqrt{Dt})$.

The "break through" time of diffusing H_2 is ∿150 h which is in good agreement with the experimental plot in figure 4.

At equilibrium the diffusive transport of hydrogen is given by the equation

$$N_f = [dH_2/dt] = A \cdot D_e \cdot C_i / \mathcal{X}$$

where N_f is the flow rate of diffusing H_2

- A is the geometrical area
- C_i is the H_2 concentration in the irradiated volume
- $\mathcal{X}$ is the thickness of the bentonite cylinder
- $D_e = \varepsilon \cdot \bar{D}$ is the effective diffusivity
- ε is the porosity

Using the following values $A = 19.63$ cm^2, $x = 1.4$ cm, $D_e = 1.8 \cdot 10^{-7}$ cm$^2 \cdot$sec^{-1}, $N_f = 4.7 \cdot 10^{-14}$ mol$\cdot$sec^{-1}, ie $3.8 \cdot 10^{-6}$ cm$^3 \cdot$h^{-1} (from figure 4) and H_2 solubility in water $0.9 \cdot 10^{-3}$ mol$\cdot$dm^{-3} (10) the H_2 concentration in the pore water and the corresponding gas phase concentration have been calculated.

3.2 GAMMA SOURCE

The gas phase concentration in the Cs-137 experiment as function of irradiation time is shown in figure 6.

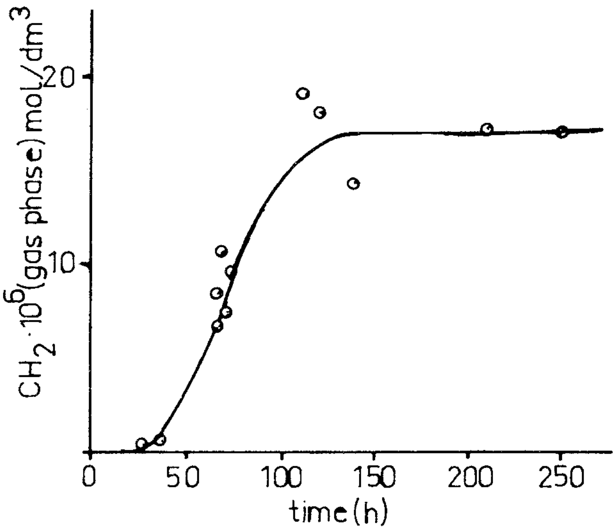

Fig. 6
H_2 concentration in gas phase vs irradiation time. Cs-137 γ-source, dose rate 0.014 rad·sec^{-1}.

3.3 HYDROGEN PRODUCTION

The equilibrium H_2 concentrations obtained with the two experimental set ups are given in table 1.

Table 1.
Hydrogen (H_2) concentration in pore water and gasphase.

Radiation source	Doserate rad·sec^{-1}	C_{H_2} (pore water) mol·dm^{-3}	C_{H_2} (gas phase) mol·dm^{-3}
Pm-147	6.11	$1.86 \cdot 10^{-5}$	$0.9 \cdot 10^{-3}$
Cs-137	0.014	$3.5 \cdot 10^{-7}$	$17 \cdot 10^{-6}$
ˣCo-60			

ˣ earlier study in this laboratory.

Whereas the H_2 concentration obtained in the low dose experiment is of the same order of magnitude as in our previous study (4), the H_2 concentration in the high dose experiment is about 30 times higher.

3.4 Fe^{2+} CONCENTRATION IN THE PORE WATER

The amount of Fe^{2+} expressed as mg Fe^{2+}/g clay obtained on analysis of the aqueous phase of clay suspensions containing varying volumes of water per unit weight dry clay at pH ∿ 6.5 is depicted in figure (7). As seen the Fe^{2+} concentration in the aqueous solutions is constant ∿ $8.6 \cdot 10^{-6}$ $mol \cdot dm^{-3}$ which is lower than the solubility of Fe^{2+}-hydroxide complexes at this pH (11).

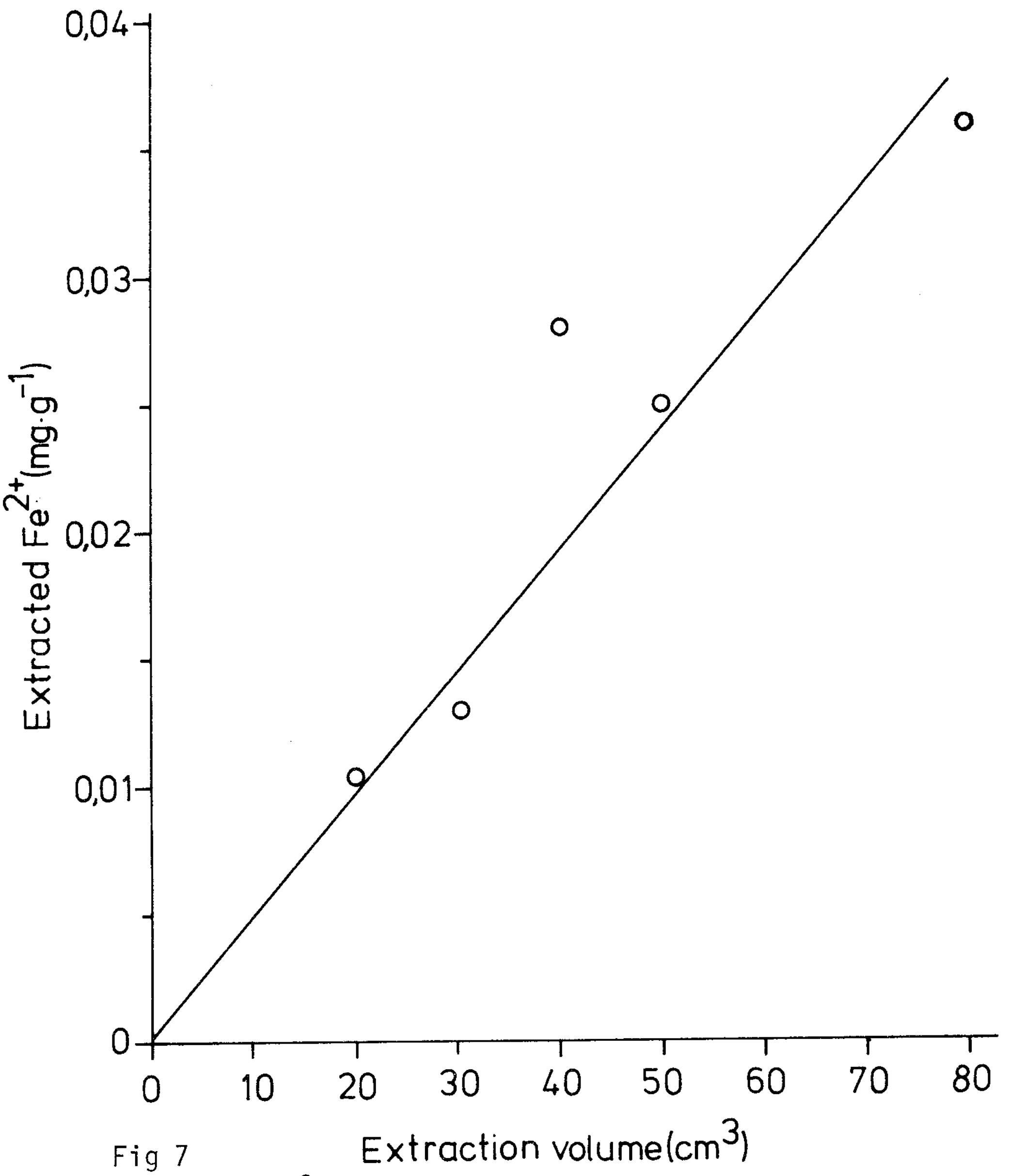

Fig 7
Extracted Fe^{2+} from 1g bentonite (Mx-80) as function of water volume (pH ~ 6).

The concentration of Fe^{2+} in clay/water slurrys containing 0.5 mol·dm^{-3} $CaCl_2$ was found to be about the same as without $CaCl_2$ indicating that the Fe^{2+} extracted most probably is not due to ion exchange, but limited by the solubility of Fe^{2+} in the pore water.

Gamma irradiation in a Co-60 cell (dose rate ∿ 300 krad·h^{-1}) to doses $\leq$ 40 Mrad produced no significant change of the Fe^{2+} concentration in the aqueous phase.

3.5 MÖSSBAUER ANALYSIS OF IRON (II) IN BENTONITE

The spectra of dry Ca (Erbslöh) and Na (MX-80) bentonites are shown in figures 8,9. The spectra are best fitted using two respectively three doublets. No spectral change was observed on addition of 20% H_2O by weight to air dry MX-80. The effects of drying and prolonged contact with synthetic ground water are shown in figures (10-13) and the spectral data are summarized in table 2.

Table 2.

Isomer shifts (δ), quadropole splittings (Δ) and relative absorption areas from Mössbauer measurements.

Bentonite	Treatment	δ mm·sec^{-1}	Δ mm·sec^{-1}	Area % of total
Ca(Erbslöh)	none	1.027	2.67	11
		0.252	0.591	89
Na	none; addi-	1.036	2.89	12.2
Mx-80	tion of 20%	0.233	0.633	71
	H_2O	1.066	2.313	16.8
	20% H_2O	1.036	2.89	6.5
	dried for	0.233	0.633	76
	1.5 h in air	1.066	2.313	16.5
	at 60°C			
	20% H_2O	1.036	2.89	0
	air dried	0.233	0.633	81
	for > 1 week	1.066	2.313	19

Table 2. cont.

Bentonite	Treatment	δ $mm \cdot sec^{-1}$	Δ $mm \cdot sec^{-1}$	Area % of total
	heated for 20 h at 425°C	0.233	0.633	100
	compacted, watersaturated for ∿ 1 year	1.036 0.233 0.975	2.89 0.633 2.15	14.7 77.2 8.1

The quadrupole splitting (Q.S.) ranging from Δ = 0.59 to 0.63 (see table 2) in Erbslöh and MX-80 corresponds well to the data obtained for octahedral Fe(III) iron by Rozenson and Heller-Kallai (12). FeS_2 and FeO(OH) may however give overlapping peaks. The absorption with quadropole splitting Δ = 2.89 is clearly caused by high spin (S = 2) Fe^{2+}, most probably $Fe(OH)_2$. The absorption with Δ = 2.13 is broad but on prolonged contact with water the band is becoming narrower and somewhat shifted. The signal may be due to Fe(II) within the actual clay-structure.

Addition of 20% H_2O followed by drying (prolonged at room temperature or briefly at 60°C) causes partial oxidation of Fe(II) in the form of $Fe(OH)_2$. All Fe(II) is oxidized on prolonged heating at 425°C.

The total iron content in bentonite has been determined by Torstenfelt et al (13) to be ∿ 3% and the divalent fraction 0.25 - 0.5. According to our Mössbauer spectroscopical analysis the Fe(II) is present in at least two different forms, one of which is $Fe(OH)_2$. The total Fe(II) content is about ~1% and the Fe(II) content accessible to dissolution and oxidation in the aqueous phase at least 0.4%. It ought, however, to be emphasized that the Fe(II) content will strongly depend on the pre-treatment of the clay. Prolonged heating at high temperature may decrease the amount of available Fe(II).

3.6 KINETIC MODEL CALCULATIONS

3.6.1 Beta source radiolysis

Calculations of hydrogen production, using the computer program described by Christensen and Bjergbakke (6) with a modified diffusion equation based on the irradiation and diffusion geometries used in the Pm-147 experiment, have been carried out. The results are listed in table 3.

Table 3.
Hydrogen production calculated by assuming homogeneous kinetics in pore water (14).

Fe^{2+} $mol \cdot dm^{-3}$	HCO_3^- $mol \cdot dm^{-3}$	$(dH_2/dt)_{diff}$ ¤ $cm^3 \cdot h^{-1}$
$3 \cdot 10^{-6}$	-	$1.8 \cdot 10^{-6}$
$3 \cdot 10^{-5}$	-	$1.3 \cdot 10^{-5}$
$3 \cdot 10^{-6}$	$2 \cdot 10^{-4}$	$1.3 \cdot 10^{-5}$
$3 \cdot 10^{-5}$	$2 \cdot 10^{-4}$	$2 \cdot 10^{-5}$
$3 \cdot 10^{-6}$	$2 \cdot 10^{-3}$	$4.7 \cdot 10^{-5}$
$3 \cdot 10^{-5}$	$2 \cdot 10^{-3}$	$4.9 \cdot 10^{-5}$

¤ Experimental value $3.8 \cdot 10^{-6}$ $cm^3 \cdot h^{-1}$

The H_2 concentration in the pore water and thereby the H_2 production is according to Christensen and Bjergbakke governed by the two competing reactions

$$\cdot OH + H_2 \longrightarrow H\cdot + H_2O \qquad (1)$$

$$\cdot OH + Fe^{2+} \longrightarrow OH^- + Fe^{3+} \qquad (2)$$

The water used in the present study is a synthetic ground water, the composition of which is given in table 4 together with the composition of natural non-saline granitic ground water.

Table 4.
Groundwater compositions.

Species	Natural $mg \cdot dm^{-3}$	Artificial[A] $mg \cdot dm^{-3}$
HCO_3^-	30-400	123
SO_4^{2-}	1-25	9.6
Cl^-	5-50	70
F^-	0.01-5	
HPO_4^{2-}	0.01-0.5	
SiO_2(tot)	5-30	12
Ca^{2+}	10-50	18
Mg^{2+}	2-20	4.3
Na^+	10-100	65
K^+	1-5	3.9
Fe^{2+}	0.5-20	

A used in the present study.

Deep granitic ground waters normally contains a fairly high concentration of hydrogen carbonate (HCO_3^-), (15) in our experiments $\sim 2 \cdot 10^{-3}$ $mol \cdot dm^{-3}$ and the reactions between HCO_3^- and radicals produced on radiolysis of water should therefore be taken into consideration, eg the reactions

$$OH + HCO_3^- \rightarrow CO_3^- + H_2O \qquad (3)$$

$$H + HCO_3^- \rightarrow CO_3^- + H_2O \qquad (4)$$

$$e_{aq}^- + CO_3^- \rightarrow CO_3^{2-} \qquad (5)$$

$$CO_3^- + CO_3^- \rightarrow CO_2 + CO_4^{2-} \qquad (6)$$

The rate constants for the reactions between $\cdot OH$ and some of the solutes present in artifical ground water Cl^-, HCO_3^-, Fe^{2+} as well as H_2 are given in table 5 below together with the $k[c]$ values calculated using the solute concentrations in table 4.

Table 5.
Reaction, concentration and rateconstant for some solutes present in artificial groundwater.

Solute	Conc $mol \cdot dm^{-3}$	Reaction	k $dm^3 mol^{-1} sec^{-1}$	k[c] sec^{-1}
Cl^-	$< 0.2 \cdot 10^{-3}$	$OH + Cl^-$	$< 10^6$	$< 2 \cdot 10^2$
HCO_3^-	$(0.5-6.5) \cdot 10^{-3}$	$OH + HCO_3 \rightarrow CO_3^- \cdot$	$3.6 \cdot 10^7$	$1.8 \cdot 10^4 - 2.4 \cdot 10$
HCO_3^-	$(0.5-6.5) \cdot 10^{-3}$	$H + HCO_3^- \rightarrow CO_3^- \cdot$	$3.4 \cdot 10^4$	$1,7-2.2 \cdot 10^2$
Fe^{2+}	$9 \cdot 10^{-5} - 3.5 \cdot 10^{-4}$	$OH + Fe^{2+} \rightarrow Fe^{3+}$	$2.3 \cdot 10^8$	$2.1 \cdot 10^4 - 8 \cdot 10^4$
H_2		$OH + H_2$	$4 \cdot 10^7$	

The importance of reaction 3 can be judged from the ratio of the k[C] values of reactions 3 and 2

$$k_3[HCO_3^-]/k_2[Fe^{2+}]$$

which is in the range (0.2 - 14).

The radical anion CO_3^- generated by the reaction between ·OH and hydrogen carbonate has a standard redox potential of 1.5 V (16) whereas the Fe^{3+}/Fe^{2+} redox potential is 0.771 V (17). The rate constants for reactions 4-6 are pH dependent and of the order of $10^7 - 10^8\ M^{-1} sec^{-1}$ and the CO_3^- radical most probably disappears by reacting with Fe^{2+}.

The hydrogen production obtained with the Pm-147 source corresponds rather well to the production calculated assuming Fe^{2+} $8 \cdot 10^{-6}$ and $HCO_3^- \approx 0\ mol \cdot dm^{-3}$.

The calculated H_2 concentration is however much higher than previously obtained in experiments using distilled water and Co-60 γ-irradiation (4) with higher dose rate as used in the present Pm-147 experiment . It is therefore reasonable to assume that the Fe^{2+} concentration in the pore water is lower than the concentration obtained in the aqueous phase after centrifugation of the clay-slurry.

Based on this assumption the higher H_2 concentration obtained in this study may be due to the increased ·OH scavenging by the HCO_3^- ion. The HCO_3^- concentration in the pore water is not known but as the clay is a cation exchanger with low anion exchange capacity this concentration will be much lower than in the ground water.

A rough estimate of the Fe^{2+} and HCO_3^- concentration in the clay pore water can be obtained based on the following arguments. The total rate of OH-scavenging can be expressed as $\Sigma k\ c = k_2[Fe^{2+}] + k_3[HCO_3^-]$ when k_2 and k_3 are the rate constants for reactions 2 and 3 respectively and $[Fe^{2+}]$ and $[HCO_3^-]$ the concentrations.

The calculated H_2 production is plotted vs $\Sigma k \cdot c$ in figure 14.

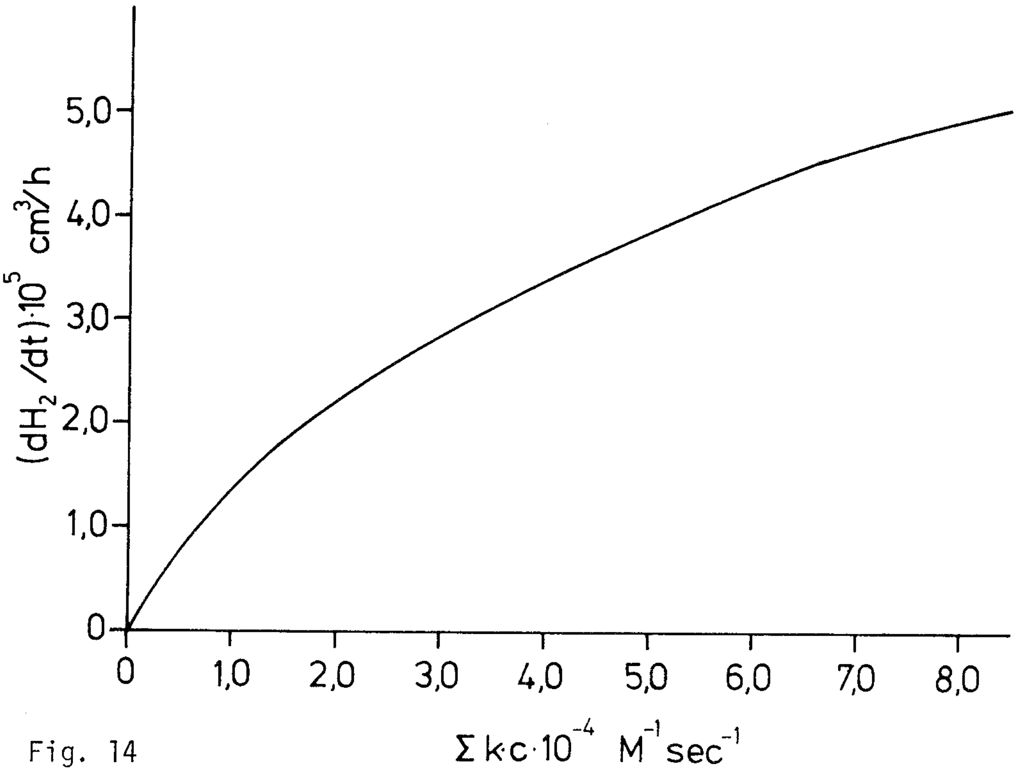

Fig. 14

Calculated H_2 production as function of the overall reaction rate of the OH scavengers Fe^{2+} and HCO_3^- $\Sigma kc = k_2 \cdot [Fe^{2+}] + k_3[HCO_3^-]$.

From our earlier experiments with distilled water (4) the gas phase concentration was found to be $\sim$ 28 $\mu mol \cdot dm^{-3}$.
This corresponds to a $\Sigma k\ c$ value of 74.7 $M^{-1} sec^{-1}$ and a Fe^{2+} concentration of $2.2 \cdot 10^{-7}$ $mol \cdot dm^{-3}$. In the present Pm-147 experiments the H_2 production of $3.6 \cdot 10^{-6}$ $cm^3 \cdot h^{-1}$ corresponds to a calculated $\Sigma k\ c$ value of $0.24 \cdot 10^4$. Assuming the Fe^{2+} concentration to be $2.2 \cdot 10^{-7}$ $mol \cdot dm^{-3}$ the HCO_3^- concentration is calculated from the expression

$$0.24 \cdot 10^4 = k_2 \cdot 2.2 \cdot 10^{-7} + k_3 [HCO_3^-]$$

to be $6.5 \cdot 10^{-5}$ $mol \cdot dm^{-3}$.

3.6.2 Gamma source radiolysis

The much lower equilibrium concentration obtained in the low dose rate Cs-137 experiments indicates a strong dose rate dependence. A corresponding dose rate dependence of the H_2 production have also been obtained in the calculations of Christensen and Bjergbakke.

4 CONCLUSIONS

The hydrogen production i e the amount of hydrogen (H_2) diffusing out of irradiated bentonite is proportional to the diffusivity and concentration of hydrogen in the bentonite pore water at radiolytic equilibrium. The hydrogen production depends on dose rate and decreases sharply at low dose rates.

At high dose rates the hydrogen concentration at radiolytic equilibrium depends strongly on the concentration of $\cdot OH$ scavengers i e Fe^{2+} and HCO_3^- in ground water. Increasing concentrations of Fe^{2+} and/or HCO_3^- give increasing production.

The hydrogen production and time for "break through" can be calculated using a homogeneous kinetic reaction model expressing the diffusion as a hydrogen consuming reaction.

The overall redox-buffer capacity of the bentonite expressed as the Fe(II) accessible as Fe^{2+} ions in pore water is at least 0,4% of the bentonite by weight. This corresponds to 0,13 $mol \cdot dm^{-3}$ of compacted (= 2,1 $kg \cdot dm^{-3}$) bentonite.

Acknowledgements

We would like to express our gratitude to Drs H Christensen and E Bjergbakke for carrying out the calculations and to Drs J Blomqvist and V Helgeson for the Mössbauer measurements.

References:

1. V I Spitsyn, B D Baluhova and M K Savushkina
"Influence of Irradiation with Gammaquanta and Beam of Accelerated Electrons on the Sorption Parameters of Clay Minerals of the Montmorillointe Group", in S Topp (Ed.) Scientific Basis for Nuclear Waste Management, Vol 4, Elsevier, NY (1982) p. 703.

2. H Christensen
Bedömning av radiolys i grundvatten.
KBS-Technical report 78.

3. H Christensen
γ-radiolysis of organic compounds and α-radiolysis of water.
KBS-Technical report 114.

4. T E Eriksen and J Lind
Mätning av radiolytiskt bildat vätgas i bentonit.
KTH, Stockholm 1978-12-01 (in Swedish).

5. I Neretnieks
The movement of a redox front downstream from a repository for nuclear waste.
KBS-Technical report 82-16.

6. H Christensen and E Bjergbakke
Radiolysis Of Ground Water From HLW Stored In Copper Canisters.
KBS-Technical report 82-02.

7. N W Holm and R J Berry (Eds)
Manual on Radiation Dosimetry.
Marcel Decker Inc NY 1970 p. 313.

8. Z Gerstl and A Banin
Fe^{2+}-Fe^{3+} transformation in clay and resin ion-exchange systems.
Clay and Clay Minerals 1980, 28:5, 335.

9. W B Fortune and M G Mellon
Determination of iron with O-phenanthronine.
Anal Chem 1938, 10, 60.

10. Handbook of Chemistry and Physics
46th Ed. p. B-178.

11. G Hägg
Kemisk reaktionslära, 7th Ed, Almqvist & Wiksell 1965, p. 158.

12. I Rozenson and L Heller Kallai
Reduction and oxidation of Fe^{3+} in diotahedral smectites III oxidation of octahedral iron in montmorillointe.
Clay and Clay Minerals 1978, 26:2, 88.

13. B Torstenfelt, B Allard, W Johansson and T Ittner
Iron content and reducing capacity of granites and bentonite.
(Report in preparation).

14. H Christensen, E Bjergbakke
Radiolysis of bentonite/water mixtures.
Studsvik-Technical Report NW-83/489
1983-06-01.

15. B Allard
On the pH-buffering effects of the CO_2-CO_3^{2-} system in deep ground waters.
KBS-Technical report 82-25.

16. A Henglein
Pulse radiolysis and polarography, p. 218 in Ed. S J Bard, Electroanalytical Chemistry, Vol 9, Marcel Decker 1976.

17. G Hägg
Kemisk reaktionslära, Almqvist & Wiksell, 1965 p. 180.

APPENDIX I

Choice of H_2 diffusion and Fe^{2+} solubility parameters.

Diffusivity: The diffusivity of H_2 in compacted bentonite has been determined by Neretnieks and Skagius (1) to be $1.8 \cdot 10^{-7}$ $cm^2 \cdot sec^{-1}$ based on geometrical area and a H_2 solutiblity of $0.8 \cdot 10^{-3}$ $mol \cdot dm^{-3}$. In similar steady state diffusion experiments Eriksen and Jacobsson (2) obtained $D_e = 0.36 \cdot 10^{-7}$ $cm^2 \cdot sec^{-1}$.

The hold up time i e the time obtained from the crossing of the prolonged steady-state straight line with the time axis is

$$t_c = d^2/6\bar{D}$$

where $\bar{D}$ is the diffusivity, d is the thickness of the bentonite layer, i e the time lag is proportional to the square of the clay-thickness, proportional to the diffusion coefficient and independent of crossreaction and tracer concentration. The diffusion coefficients $\bar{D}$ calculated from Neretnieks and our experimental data are $1.6 \cdot 10^{-7}$ and $4.11 \cdot 10^{-7}$ $cm^2 \cdot sec^{-1}$ respectively. If the H_2 diffusion is assumed to take place in the pore water only and no adsorption takes place, there is in both experiments a discrepancy between the diffusivities calculated from steady state transport and the hold up time. In both experimental set ups metallic filters were used as interphase between the bentonite and water and this will give rise to too long hold up times the effect being more pronounced in Neretnieks experiments due to a thinner clay disc. From the hold up time obtained in our experiments the diffusivity D_e is related to $\bar{D}$ according to the equation

$$D_e = \bar{D} \cdot \varepsilon$$

The porosity corresponding to the clay density 2.1 $kg \cdot dm^{-3}$ is ~ 0.35 and thus $D_e \sim 1.45 \cdot 10^{-7}$ $cm^2 \cdot sec^{-1}$. The "best value" from the two published reports is taken to be $1.8 \cdot 10^{-7}$ $cm^2 \cdot sec^{-1}$.

Fe^{2+}, Fe^{3+} solubility.

The pH of the porewater is assumed to be (8.2-8.8). The solubility of $Fe(OH)_2$ in water within this pH domain is $\sim 3.10^{-4}-10^{-5}$ $mol\cdot dm^{-3}$ (4).

The Fe^{2+} concentration in the aqueous phase of a bentonite suspension at pH $\sim$ 6 (HCl) was found to be $8.6\cdot 10^{-6}$ $mol\cdot dm^{-3}$ and independent of solution/clay ratio in the range (10-80 cm^3)/g indicating that the concentration is determined by the Fe^{2+} solubility in the pore water. Fe^{2+} concentrations of $3\cdot 10^{-6}$ and $3\cdot 10^{-5}$ $mol\cdot dm^{-3}$ were used in the calculations.

References:

1) I Neretnieks and C Skagius,
Diffusionsmätningar av metan och väte i våt lera,
KBS-Technical report 86 (1978).

2) T E Eriksen, A Jacobsson
Diffusion of hydrogen, hydrogen sulfide and large molecular weight anions in bentonite.
KBS-Technical report 82-17.

3) J Crank,
The mathematics of diffusion,
Oxford University Press, 1957, p.48.

4) Hägg,
Kemisk reaktionslära
Almqvist & Wiksell 1965

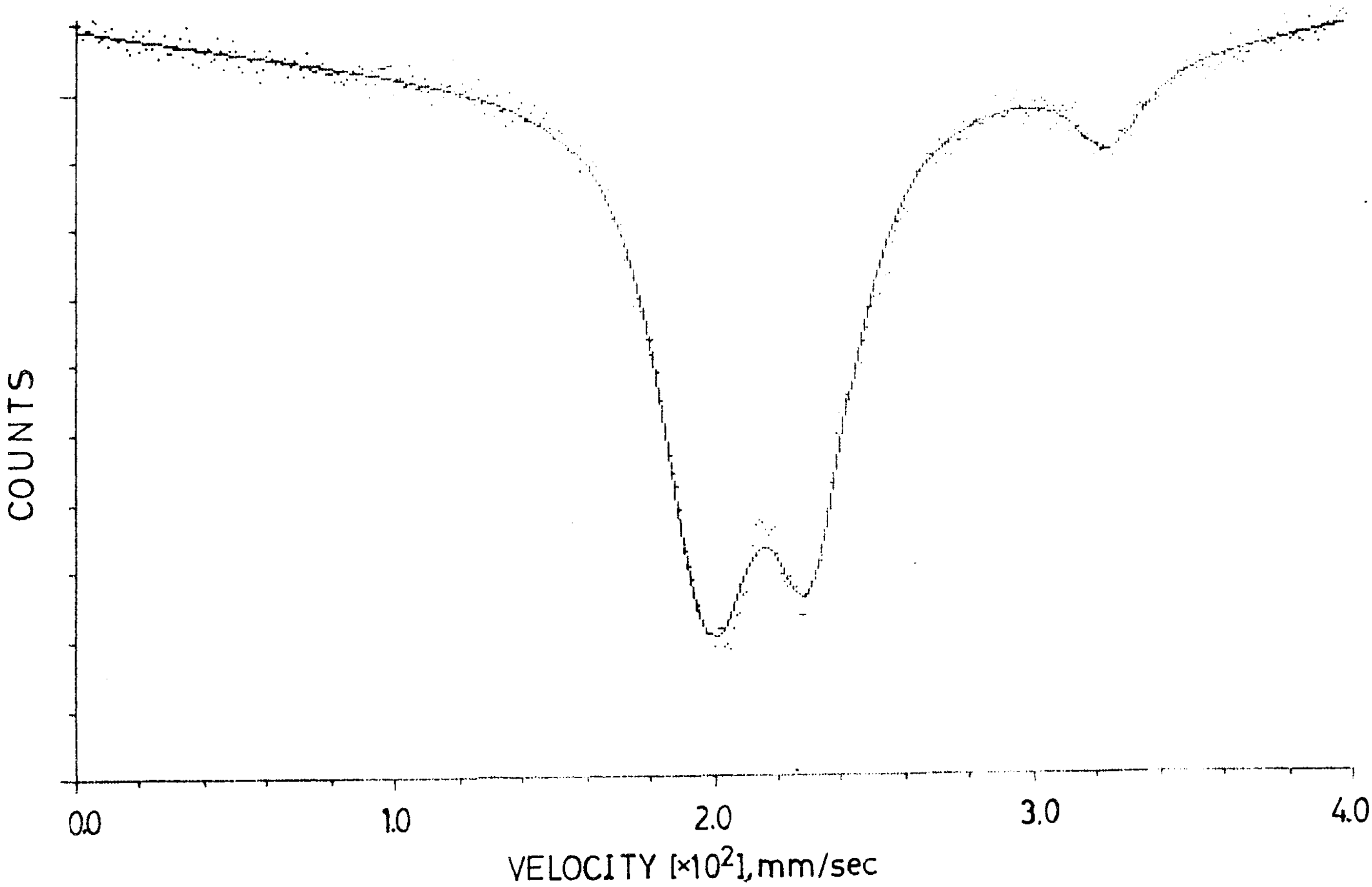

Fig 8.
Mössbauer spectrum of dry Ca-bentonite
(Erbslöh).

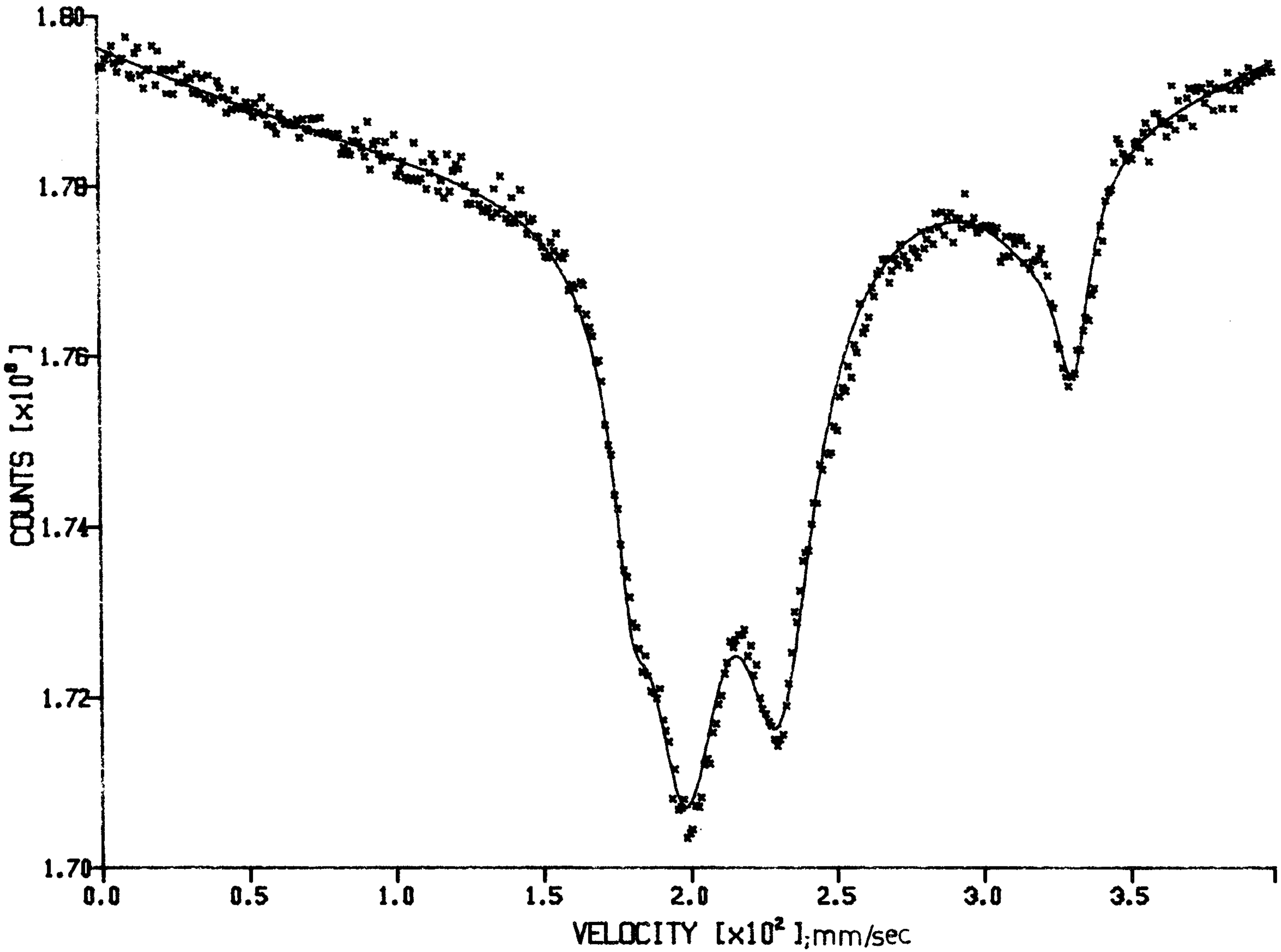

Fig 9.
Mössbauer spectrum of dry Na-bentonite Mx-80.

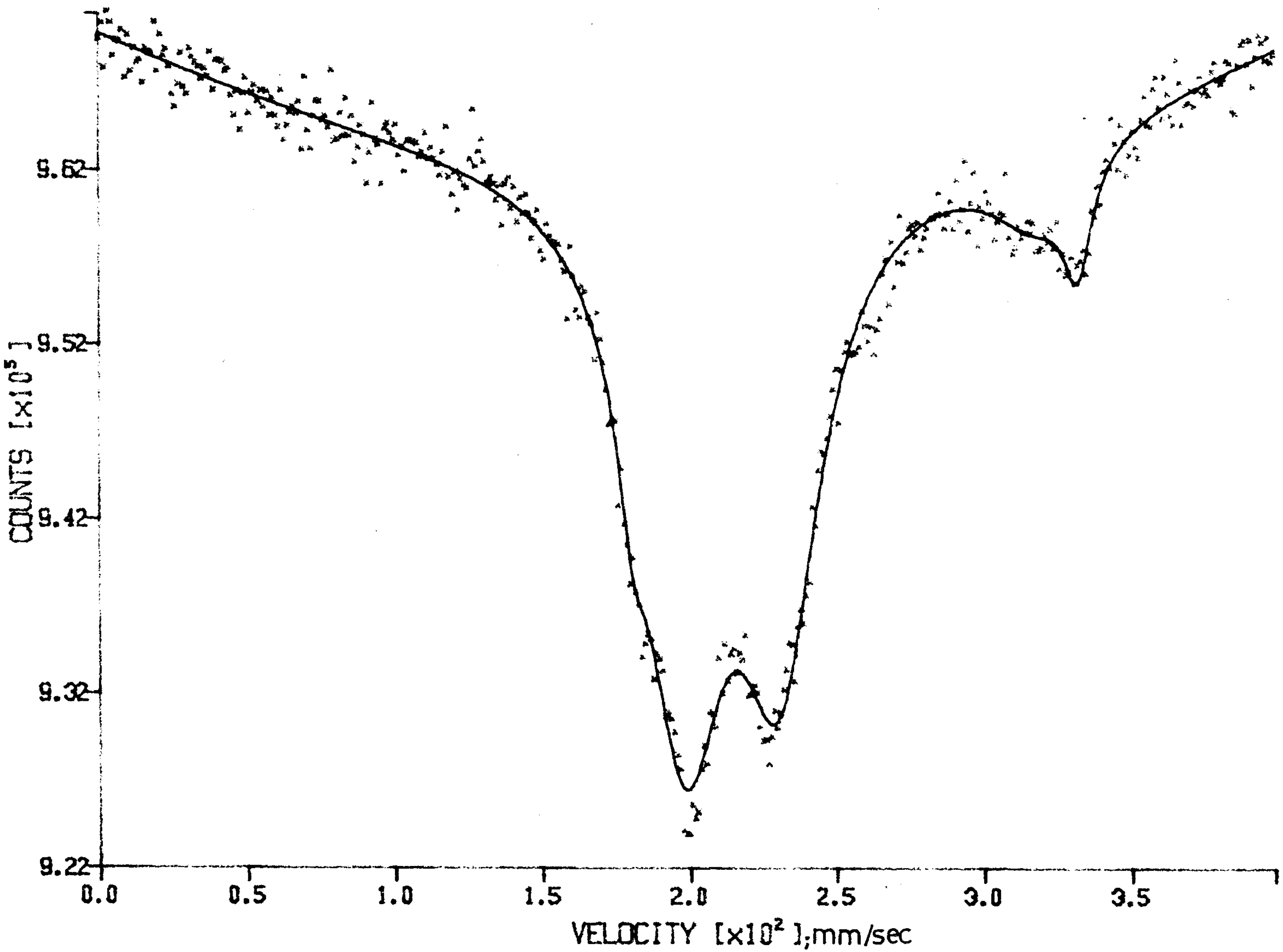

Fig 10.
Mössbauer spectrum of Mx-80. 20% H_2O added,
dried in air for 1.5 h at 60°C.

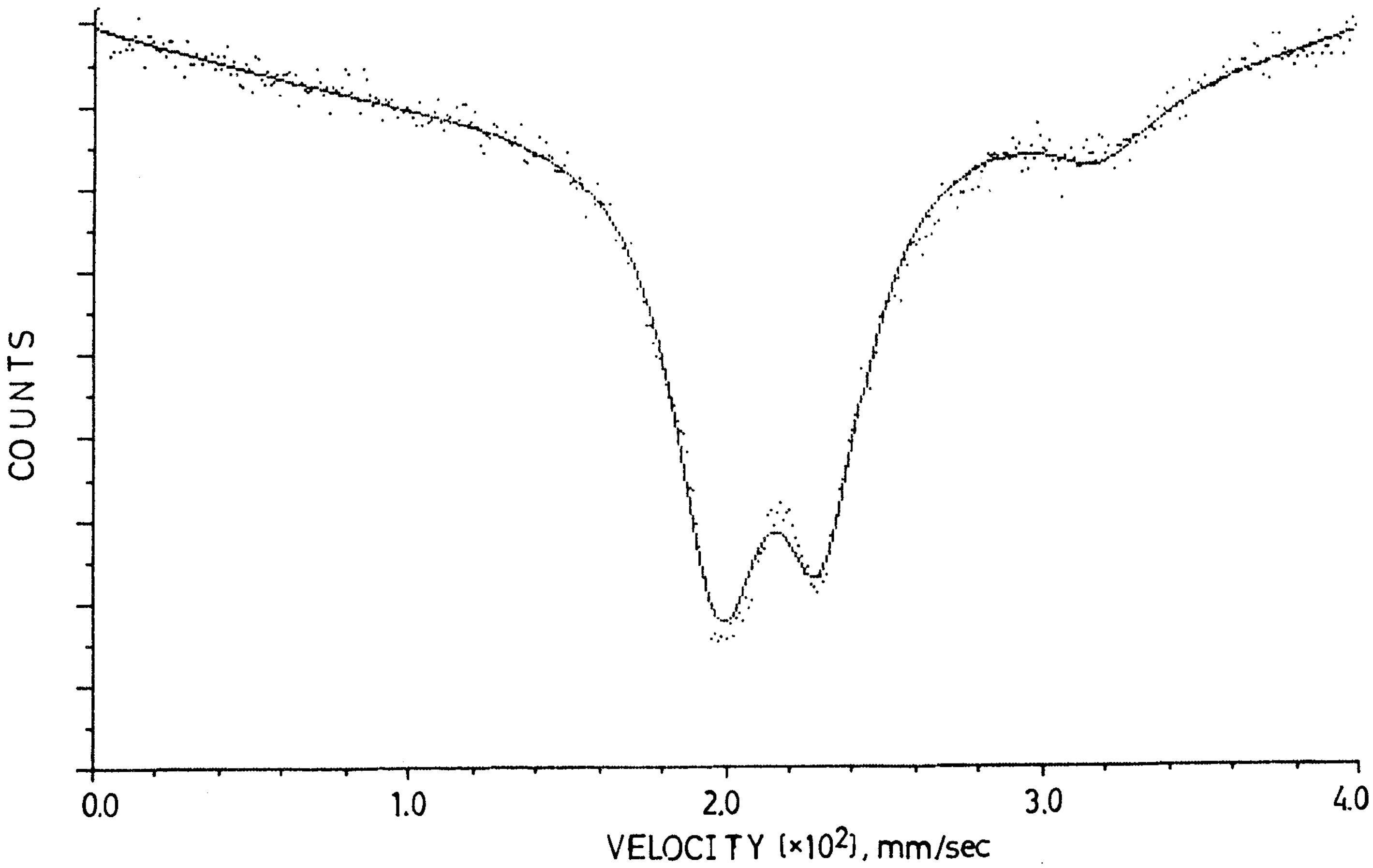

Fig 11.
Mössbauer spectrum of Mx-80; 20% H_2O added, dried in air at ambient temperature for ~ 2 weeks.

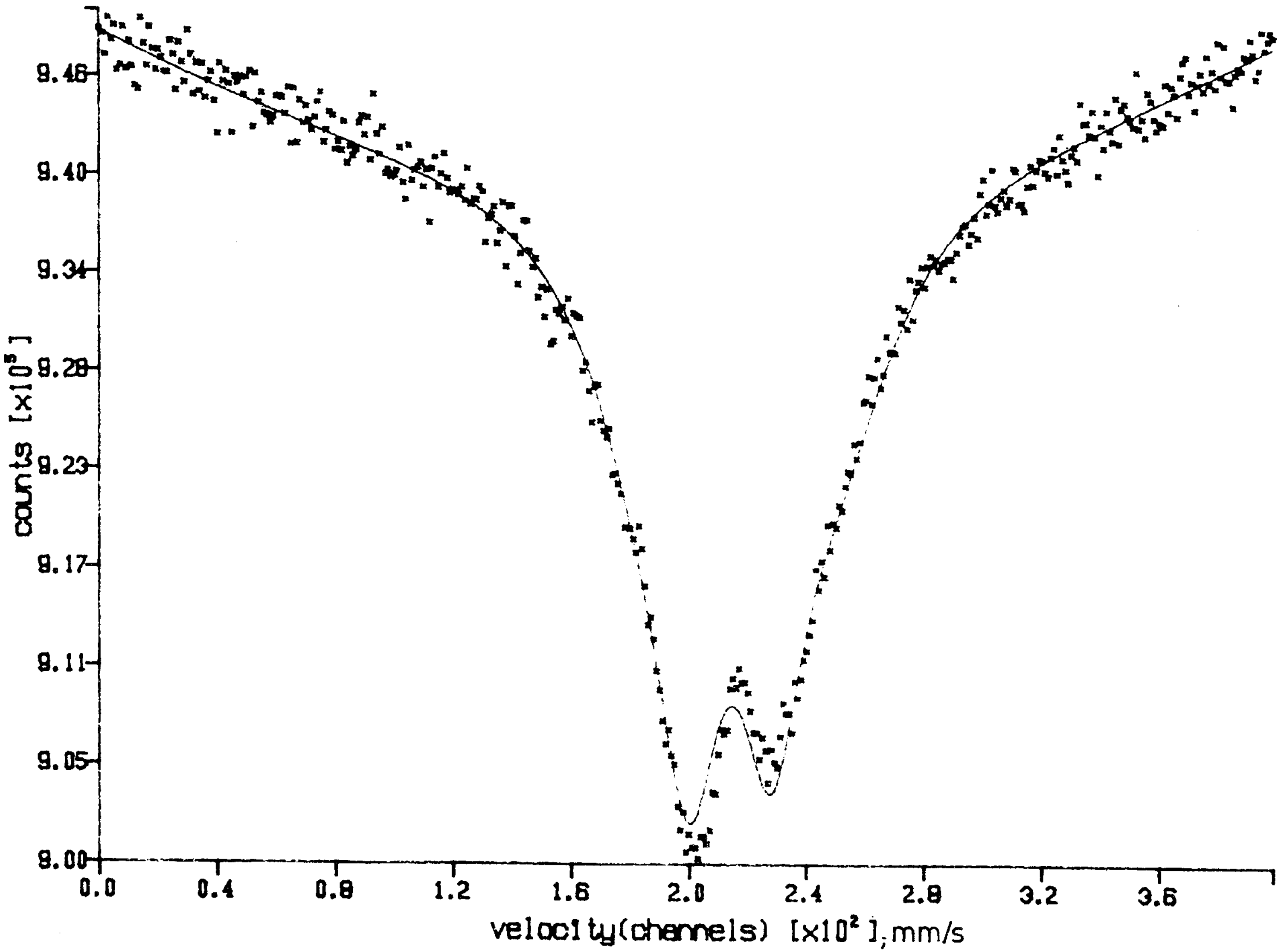

Fig 12.
Mössbauer spectrum of Mx-80, dried for 24 h at 425°C.

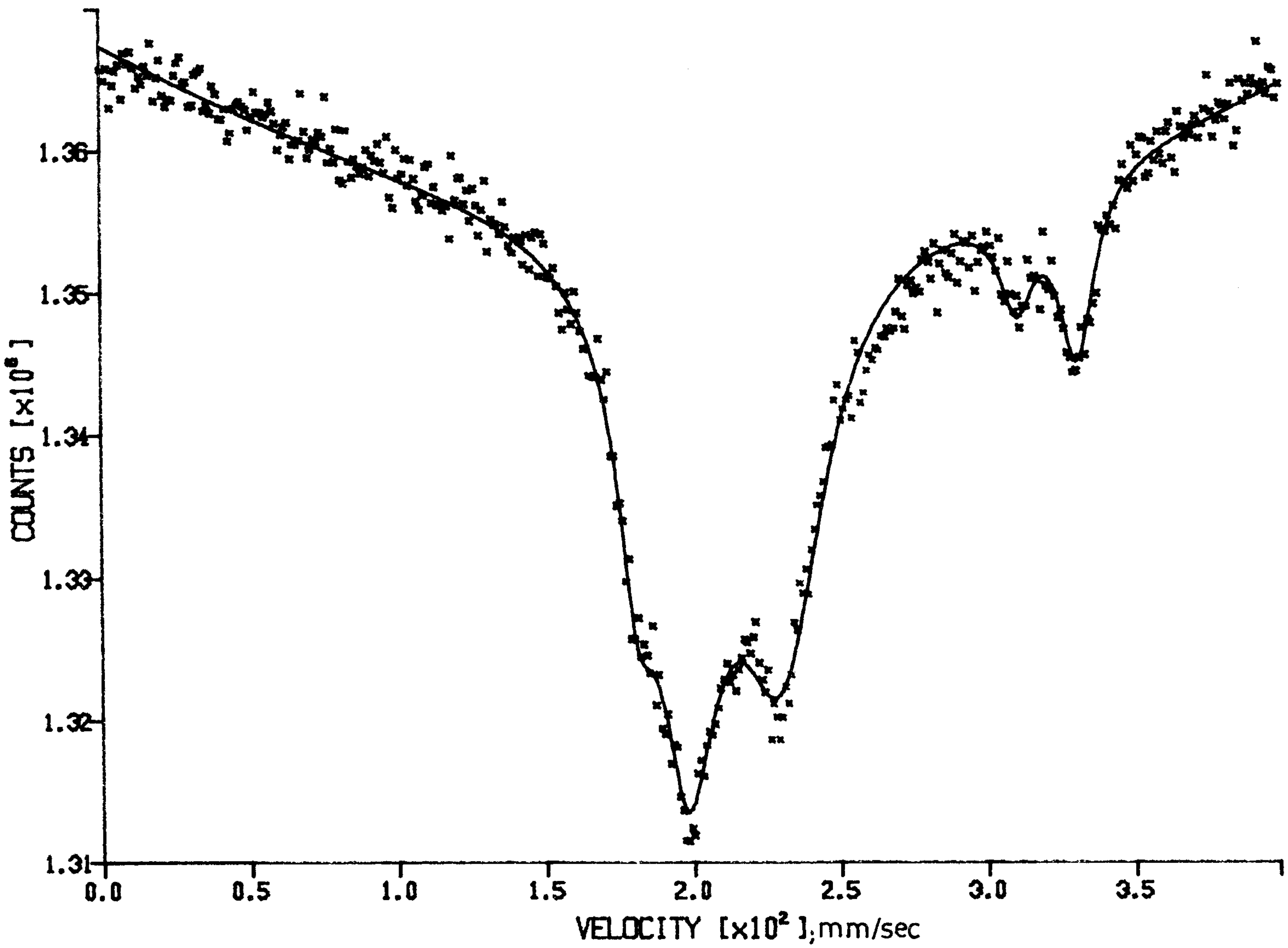

Fig 13.
Mössbauer spectrum of Mx-80 after 1 years contact with air saturated synthetic ground water in a swelling pressure oedometer.

LIST OF KBS's TECHNICAL REPORTS

TR 83-03 Smectite alteration
Proceedings of a colloquium at State University of New York at Buffalo, May 26-27, 1982
Compiled by Duwayne M Anderson
State University of New York at Buffalo
February 15, 1983

TR 83-04 Stability of bentonite gels in crystalline rock - Physical aspects
Roland Pusch
Division Soil Mechanics, University of Luleå
Luleå, Sweden, 1983-02-20

TR 83-05 Studies in pitting corrosion on archeological bronzes - Copper
Åke Bresle
Jozef Saers
Birgit Arrhenius
Archaeological Research Laboratory
University of Stockholm
Stockholm, Sweden 1983-01-02

TR 83-06 Investigation of the stress corrosion cracking of pure copper
L A Benjamin
D Hardie
R N Parkins
University of Newcastle upon Tyne
Department of Metallurgy and Engineering Materials
Newcastle upon Tyne, Great Britain, April 1983

TR 83-07 Sorption of radionuclides on geologic media - A literature survey. I: Fission Products
K Andersson
B Allard
Department of Nuclear Chemistry
Chalmers University of Technology
Göteborg, Sweden 1983-01-31

TR 83-08 Formation and properties of actinide colloids
U Olofsson
B Allard
M Bengtsson
B Torstenfelt
K Andersson
Department of Nuclear Chemistry
Chalmers University of Technology
Göteborg, Sweden 1983-01-30

TR 83-09 Complexes of actinides with naturally occurring organic substances - Literature survey
U Olofsson
B Allard
Department of Nucluear Chemistry
Chalmers University of Technology
Göteborg, Sweden 1983-02-15

TR 83-10 Radiolysis in nature:
Evidence from the Oklo natural reactors
David B Curtis
Alexander J Gancarz
New Mexico, USA February 1983

TR 83-11 Description of recipient areas related to final storage of unreprocessed spent nuclear fuel
Björn Sundblad
Ulla Bergström
Studsvik Energiteknik AB
Nyköping, Sweden 1983-02-07

TR 83-12 Calculation of activity content and related properties in PWR and BWR fuel using ORIGEN 2
Ove Edlund
Studsvik Energiteknik AB
Nyköping, Sweden 1983-03-07

TR 83-13 Sorption and diffusion studies of Cs and I in concrete
K Andersson
B Torstenfelt
B Allard
Department of Nuclear Chemistry
Chalmers University of Technology
Göteborg, Sweden 1983-01-15

TR 83-14 The complexation of Eu(III) by fulvic acid
J A Marinsky
State University of New York at Buffalo, Buffalo,NY
1983-03-31

TR 83-15 Diffusion measurements in crystalline rocks
Kristina Skagius
Ivars Neretnieks
Royal Institute of Technology
Stockholm, Sweden 1983-03-11

TR 83-16 Stability of deep-sited smectite minerals in crystalline rock - chemical aspects
Roland Pusch
Division of Soil Mechanics, University of Luleå
1983-03-30

TR 83-17 Analysis of groundwater from deep boreholes in Gideå Sif Laurent
Swedish Environmental Research Institute
Stockholm, Sweden 1983-03-09

TR 83-18 Migration experiments in Studsvik
O Landström
Studsvik Energiteknik AB
C-E Klockars
O Persson
E-L Tullborg
S Å Larson
Swedish Geological
K Andersson
B Allard
B Torstenfelt
Chalmers University of Technology
1983-01-31

TR 83-19 Analysis of groundwater from deep boreholes in Fjällveden
Sif Laurent
Swedish Environmental Research Institute
Stockholm, Sweden 1983-03-29

TR 83-20 Encapsulation and handling of spent nuclear fuel for final disposal
1 Welded copper canisters
2 Pressed copper canisters (HIPOW)
3 BWR Channels in Concrete
B Lönnerberg, ASEA-ATOM
H Larker, ASEA
L Ageskog, VBB
May 1983

TR 83-21 An analysis of the conditions of gas migration from a low-level radioactive waste repository
C Braester
Israel Institute of Technology, Haifa, Israel
R Thunvik
Royal Institute of Technology
November 1982

TR 83-22 Calculated temperature field in and around a repository for spent nuclear fuel
Taivo Tarandi, VBB
Stockholm, Sweden April 1983

TR 83-23 Preparation of titanates and zeolites and their uses in radioactive waste management, particularly in the treatment of spent resins
Å Hultgren, editor
C Airola
Studsvik Energiteknik AB
S Forberg, Royal Institute of Technology
L Fälth, University of Lund
May 1983

TR 83-24 Corrosion resistance of a copper canister for spent nuclear fuel
The Swedish Corrosion Research Institute and its reference group
Stockholm, Sweden April 1983

TR 83-25 Feasibility study of EB welding of spent nuclear fuel canisters
A Sanderson, T F Szluha, J Turner
Welding Institute
Cambridge, United Kingdom April 1983

TR 83-26 The KBS UO_2 leaching program
Summary Report 1983-02-01
Ronald Forsyth, Studsvik Energiteknik AB
Nyköping, Sweden February 1983

TR 83-27 Radiation effects on the chemical environment in a radioactive waste repository
Trygve Eriksen
Royal Institute of Technology, Stockholm
Arvid Jacobsson
University of Luleå, Luleå
Sweden 1983-07-01